20% Efficient Screen-Printed n-Type Solar Cells Using a Spin-On Source and Thermal Oxide/Silicon Nitride Passivation

Arnab Das, Kyungsun Ryu, and Ajeet Rohatgi, *Fellow, IEEE*

***Abstract*—N-type Si cells offer a compelling alternative to p-type cells to achieve high, stabilized cell efficiencies because they do not suffer from light-induced degradation. However, the most common dielectric materials that are used to passivate the n^+ emitters of p-type cells—thermal SiO_2 and SiN_X—have historically provided poor passivation of the p^+ emitters required for n-type cells. In this paper, we demonstrate that a thin thermal-SiO_2/SiN_X stack can, when appropriately fired, provide similar passivation on both p^+ and n^+ surfaces. Passivation studies on textured, SiO_2/SiN_X passivated p^+-Si surfaces indicate that a high-temperature firing cycle is the most important step to achieving high-quality passivation and that the positive charge in the dielectric stack may have little detrimental effect on industrial-type, high surface concentration emitters. In addition, the suitability of spin-on boric acid sources for forming uniform, well-passivated p^+ emitters on textured surfaces was studied. This passivation scheme and spin-on boron source were used to achieve 4-cm^2 screen-printed n-type cells with efficiencies over 20% and open-circuit voltages up to 650 mV.**

***Index Terms*—Boron, diffusion processes, passivation, photovoltaic cells.**

I. Introduction

BORON-DOPED p-type Si is currently the substrate material of choice for fabricating crystalline Si solar cells. Several high-efficiency p-type cell structures exist which use a variety of processing techniques, such as liquid source diffusion, solid source diffusion, laser doping and ion implantation for junction/ back-surface field (BSF) formation, and photolithography, screen-printing, ink/aerosol jet printing, and plating for contact formation [1]–[5]. There is, however, a common feature of many of the best p-type cells—the use of thermal oxide (SiO_2) and/or silicon nitride (SiN_X) for passivating the n^+ emitter. Several studies exist which characterize the passivation qualities of SiO_2 and SiN_X on heavily doped n^+ surfaces [6]–[9]. Unfortunately, cells fabricated on p-type Cz substrates are known to be susceptible to light-induced degradation (LID) [10]. Furthermore, modeling and simulation work has indicated that higher efficiency cell structures can suffer significantly higher losses from LID [11].

N-type cells offer a way of avoiding the efficiency penalty associated with LID. Unfortunately, thermal SiO_2 and SiN_X—which provide excellent passivation of the n^+ emitters of p-type cells—have historically had problems providing passivation of similar quality and stability on the p^+ emitters required for n-type cells [12]–[18]. Prior work has shown that SiN_X passivation of planar p^+-Si surfaces results in extremely high saturation current densities J_0 of 800–2000 fA/cm^2 [12], [15]. This sets a very low V_{OC} ceiling of just ~630 mV. While thermal SiO_2 provides much better passivation on planar p^+ surfaces, several authors have reported that texturing the surface increases the surface recombination velocity S by approximately an order of magnitude [16], [17]. Additionally, the passivation of some of the highest quality thermal SiO_2 grown on p^+-Si has been reported to be unstable on both planar and textured p^+ surfaces over a period of 2–3 years [12], [14].

Higher recombination activity of defects at the p^+-Si/SiO_2 and p^+-Si/SiN_X interfaces and the fixed positive charge in SiO_2 and SiN_X have been cited as being responsible for their poor passivation quality on p^+ surfaces [12], [18]. Fired, chemically grown SiO_2/SiN_X stacks and the negatively charged Al_2O_3 have proven more successful at passivating p^+-Si surfaces, while thermal SiO_2/SiN_X stacks have had mixed success [18]–[22]. In this paper, we have attempted to separate and quantify the impact that hydrogenation, charge, and firing have on the passivation quality of both planar and textured p^+-Si surfaces using thermal SiO_2/SiN_X stacks. In addition, a spin-on boric acid solution was used in these studies in order to examine the potential of spin-on sources, which are generally safer and less toxic than the more common BBr_3, BCl_3, and doped solid sources used to form high-quality emitters for n-type solar cells [23], [24].

II. Experimental Details

The structure of the ~3 Ω·cm float-zone (FZ) n-type cells (4-cm^2 area) fabricated in this study is shown in Fig. 1. After random pyramid texturing of both sides of the wafers and cleaning, a 45–50 Ω/□ emitter was formed using a spin-on boric acid solution as the boron source [15]. A subsequent $POCl_3$ diffusion was used to form the ~70 Ω/□ BSF with back-to-back loading to prevent counterdoping of the boron emitter. The borosilicate glass layer that forms during the boron diffusion was also left intact through the $POCl_3$ diffusion step to provide further protection of the emitter. After an HF dip to remove the

Manuscript received July 22, 2011; revised October 5, 2011; accepted October 7, 2011. Date of publication November 11, 2011; date of current version December 27, 2011.

The authors are with the School of Electrical and Computer Engineering, Georgia Institute of Technology, Atlanta, GA 30332-0250 USA (e-mail: arnab.das@gatech.edu; ksryu@gatech.edu; ajeet.rohatgi@ece.gatech.edu).

Color versions of one or more of the figures in this paper are available online at http://ieeexplore.ieee.org.

Digital Object Identifier 10.1109/JPHOTOV.2011.2172189

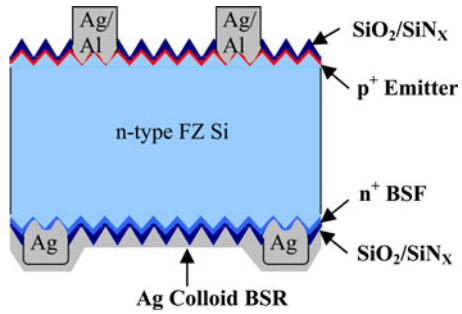

Fig. 1. Structure of thermal-SiO_2/SiN_X passivated n-type cell with screen-printed contacts.

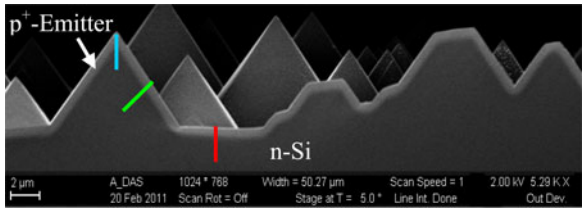

Fig. 2. SEM image of a p^+ emitter formed on a textured surface using a spin-on boric acid source. Pixel intensity profiles of the marked regions are shown in Fig. 3.

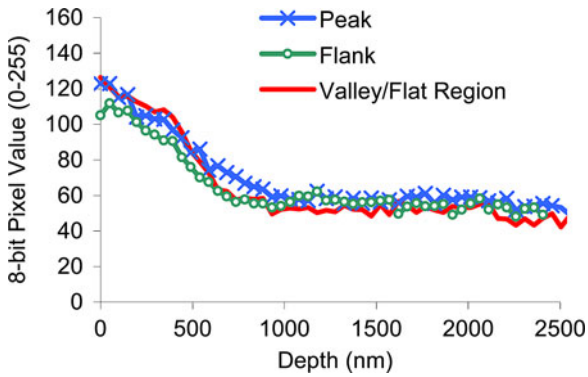

Fig. 3. Pixel intensity profile of the peak, flank, and valley regions marked in Fig. 2

borosilicate and phosphosilicate glasses, the wafers were passivated on both sides with a thin (~10–15 nm) thermal SiO_2 layer. This oxide layer was then capped with a low-frequency plasma-enhanced chemical vapor deposited (LF-PECVD) SiN_X film deposited using a Centrotherm PECVD reactor. The wafers were metalized by screen-printing Ag/Al and Ag pastes on the front (grid pattern) and rear (point contact pattern) sides, respectively, and co-fired at a temperature of ~750 °C. A conductive, light-scattering Ag colloid film was then applied to the rear surface with a brush to electrically connect the rear point contacts after firing. This layer also serves as a Lambertian back-surface reflector (BSR). Details of the characteristics of this film have previously been published [25]. The bulk lifetime of cells was determined via the quasi-steady-state photoconductivity (QSS-PC) method by etching the samples down to the bulk, cleaning the wafer and passivating both surfaces with I_2/Methanol [26].

Passivation quality at various steps of the fabrication sequence was tracked using implied V_{OC} and saturation current density J_0 measurements via the QSS-PC and transient photoconductivity decay (Transient-PCD) methods, respectively [26], [27]. The implied V_{OC} measurements were made on unmetallized cells (see structure in Fig. 1). For J_0 measurements, symmetrically diffused and passivated $p^+/n/p^+$ samples were prepared on 500–700 Ω·cm n-type FZ wafers. These samples were split into two groups: double-side textured and double-side planar, with sample size of 48 and 10, respectively. For comparison, a double-side textured $n^+/n/n^+$ J_0 sample was also fabricated. While the diffusion and passivation steps that are used to prepare the J_0 samples were identical to those used for cell processing, the $p^+/n/p^+$ J_0 wafers only went through the $POCl_3$ thermal cycle with no phosphorous diffusion occurring. The difference in the sheet resistance of the planar and textured p^+ samples was 3 Ω/ or less as measured using a four-point probe tool. On some of the J_0 samples, a forming gas anneal (FGA) was performed for ~15 min. Such anneals were not performed at any step of the cell fabrication process. As conventional profiling methods, such as secondary ion mass spectroscopy (SIMS) have trouble with accurately profiling rough surfaces, scanning electron microscopy (SEM) was used to check both the uniformity of the spin-on emitter and to estimate the junction depth [28]. The SEM imaging was done using a Zeiss Ultra 60 FE-SEM. The charge density of the thermal SiO_2/SiN_X stacks was determined using a Semitest SCA-2500 surface charge analyzer on undiffused, planar 1.3-Ω·cm p-type FZ wafers.

III. Results and Discussion

A. Emitter Uniformity

With spin-on sources, uniformity of the diffused junction on a textured surface is a concern as discontinuities in the emitter can cause shunts after metallization and introduce uncertainty in J_0 measurements. The uniformity of the spin-on boric acid diffused emitters in this study was, therefore, checked using SEM imaging. Several samples up to ~6 cm long were imaged to allow reasonably large sections to be checked. Differences in doping concentration and dopant type show up in SEM images as a contrast difference [28]: The p^+ emitter formed using the spin-on boric acid source is clearly visible as a bright line in the SEM image in Fig. 2.

Elliot *et al.* showed that the intensity/brightness of the doped region (stored as an 8-bit pixel value in the SEM image) is directly related to the ionized p^+ dopant concentration [28]. Therefore, the "pixel intensity" profile across the p^+-n junction was extracted from the SEM images. Such profiles provide a quantitative method of estimating junction depth using SEM images, and from an examination of multiple samples, we estimate a junction depth of ~0.8 ± 0.05 µm which was fairly uniform in the peaks, valleys, and flanks of the pyramid textured surface. Profiles for the regions marked in Fig. 2 are shown in Fig. 3.

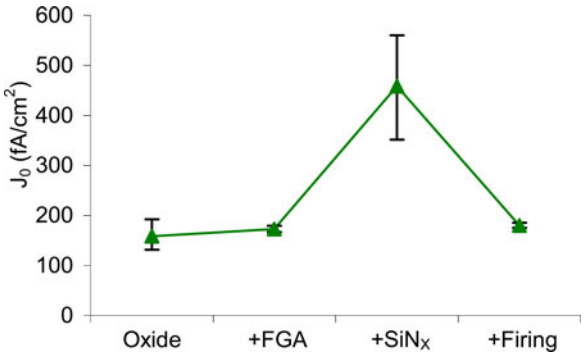

Fig. 4. J_0 of planar, boron diffused wafers at various process steps.

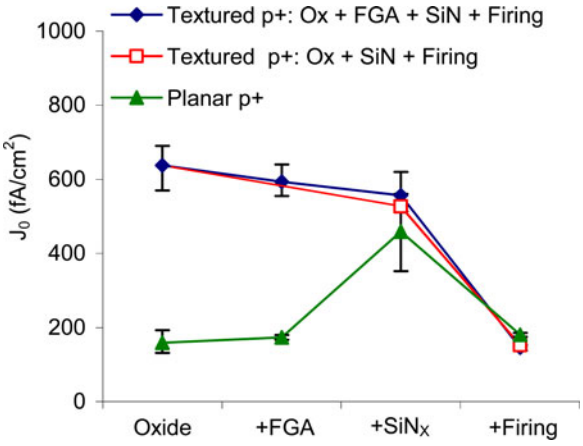

Fig. 5. J_0 of planar and textured boron diffused wafers at various process steps.

B. Surface Passivation

Fig. 4 shows the effect of various passivation steps on the J_0 of planar boron diffused surfaces. While the ~400 °C FGA step is not used in the cell fabrication sequence, it was performed on the J_0 samples to try and separate the effect of hydrogenation from the other effects of a PECVD SiN_X deposition. Both the FGA and the SiN_X deposition were performed at ~400 °C. As shown in Fig. 4, the FGA step had a negligible impact on J_0. This suggests that the thermal SiO_2-passivated planar p^+-Si surface has relatively few dangling bonds (or other sites) available for passivation by H-atoms at ~400 °C. Therefore, hydrogenation during PECVD SiN_X is unlikely to improve J_0, and instead the negative effects of this step, namely, a high positive charge in the stack (~1-2e12 cm^{-2}) and possible plasma-induced damage can be expected to dominate. The large increase in J_0 observed after SiN_X capping (see Fig. 4) matches this expected behavior. We note that even though the as-grown SiO_2/Si interface appears to be relatively free of defects that can retain hydrogen, it has been shown that ion bombardment during PECVD deposition creates a thin damaged layer at the wafer surface which can retain hydrogen [29], [30]. Therefore, some of the plasma-induced damage may be repaired *in situ* by hydrogenation; however, this effect appears to be overshadowed by the combined effects of plasma-induced damage and positive charge.

However, a very different J_0 trend was observed on identically processed textured wafers. Fig. 5 shows that the J_0 of the as-oxidized, textured p^+ surface is four to five times higher than on the counterpart planar surface. Texturing often results in increased surface recombination because of an increase in the surface area and because of the $\{1\,1\,1\}$ oriented textured surface having a larger density of dangling bonds than the planar $\{1\,0\,0\}$ orientation [7]. However, the magnitude of increase observed here is both larger than the ~1.7x increase in surface area due to texturing and larger than the increase in J_0 due to texturing seen on passivated phosphorous emitters with similar surface concentrations [7]. Why texturing a p^+ surface causes such a large increase in J_0 is not clear but, as noted in Section I, similar results have been reported earlier [13]. Based on the results on planar surfaces, SiN_X deposition might be expected to result in a further worsening of the passivation quality. However, unlike the planar case, depositing SiN_X on top of the textured SiO_2-passivated surface caused a *reduction* in J_0 (see Fig. 5). This effect, while unexpected, was found to be reproducible.

A second point of difference between the SiO_2-passivated planar and textured p^+-Si surfaces is sensitivity to hydrogenation, as seen in Fig. 5, the J_0 of the textured samples dropped after an FGA. The increased sensitivity to hydrogenation exhibited by the textured samples can be explained by assuming that (unlike the planar case) the SiO_2-passivated, *textured* p^+ surface has a significant density of unsatisfied dangling bonds which can be H-terminated by a subsequent hydrogenation step. This is a plausible explanation as $\{1\,1\,1\}$ oriented textured surfaces have a larger dangling bond density. In fact, a similar increase in sensitivity to hydrogenation is also observed when n^+-Si surfaces are textured [7]. While this theory provides a simple way of explaining why planar and textured surfaces respond differently to an FGA step, the difference observed after SiN_X capping is harder to explain as multiple processes are active during the deposition. One possible explanation is that during PECVD SiN_X deposition on textured surfaces, the increase in surface defect density due to plasma damage is outweighed by the competing reduction in surface defects by *in situ* hydrogenation of dangling bonds at the textured Si/SiO_2 interface. As the planar Si/SiO_2 interface has relatively few dangling bonds available for H-termination, the plasma-damage process dominates for planar surfaces. We note, however, that more work is needed to conclusively separate out the effects of the competing hydrogenation and plasma-damage processes. Our results here simply show the net effect of these processes on passivation quality.

Finally, firing the SiO_2/SiN_X stack resulted in a nearly four-fold reduction in J_0 on the textured wafers. The planar wafers, in contrast, improved by a factor of just 2.5, resulting in the planar and textured p^+ surfaces both having nearly identical J_0 values of ~150 fA/cm^2 after firing, which sets a V_{OC} limit of ~680 mV using the diode equation

$$V_{OC} = \frac{kT}{q} \ln\left(\frac{J_{SC}}{J_0} + 1\right) \tag{1}$$

where k, T, and q are, respectively, the Boltzmann constant, temperature, and electron charge. To our knowledge, this is the

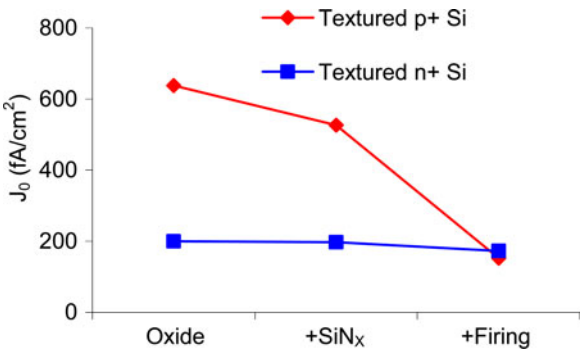

Fig. 6. Comparison of the J_0 of textured boron and phosphorous diffused wafers at the same process steps.

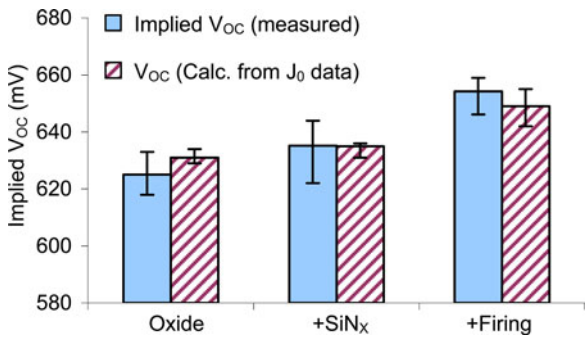

Fig. 7. V_{OC} of cell structures at various process steps as measured using the implied V_{OC} method and as calculated from J_0 data of textured samples.

first example of a passivation method that results in similar passivation quality on both textured and planar p^+ surfaces. Furthermore, the fired SiO_2/SiN_X stack provides nearly identical passivation on the textured p^+-emitter and textured n^+-BSF (see Fig. 6) used in this study. On planar wafers diffused under similar conditions, SIMS measurements showed surface concentrations of ~5e19 and ~7e19 cm^{-3} for the emitter and BSF, respectively.

Potential explanations for the large impact of firing on J_0 include release of hydrogen from the SiN_X layer, thermal annealing of surface defects, and reduction in the SiO_2/SiN_X charge density. A reduction in charge density is not supported by our measurements which show a slight increase in charge density after firing. However, the other two mechanisms have both been shown to occur during firing [30], [31]. On the planar samples, this hydrogenation/annealing effect appears to fully heal the plasma-induced damage caused by the PECVD step. The fact that the effect of firing is magnified on textured surfaces is perhaps due to dangling bonds (which were not satisfied by PECVD hydrogenation) being hydrogenated in addition to the healing of plasma-induced damage. Note from Fig. 4 that firing the SiO_2/SiN_X stack reduced the J_0 of the planar samples to a value just ~1.1x higher than that achieved with thermal SiO_2-only passivation. The fired SiO_2/SiN_X stack and the SiO_2 layer have charge density of ~2e12 and ~2e11 cm^{-3}, respectively. This suggests that for the industrial-type, high surface concentration p^+ emitter used here, the positive SiN_X charge has only a small effect on J_0.

Although the increase in surface area because of texturing might be expected to result in $J_{0,\text{textured}}$ being at least 1.7x higher than $J_{0,\text{planar}}$, this effect is suppressed for well-passivated, heavily doped emitters as recombination within the emitter starts to dominate J_0. This effect holds for both p^+ and n^+ emitters and similar results (i.e., $J_{0,\text{textured}} \approx J_{0,\text{planar}}$) have been reported for SiO_2-passivated n^+-Si emitters with surface dopant concentrations similar to our samples [7], [32].

The beneficial effect of SiN_X capping and firing on passivation quality was also seen on the implied V_{OC} of unmetallized cell wafers with textured front and rear surfaces (see Fig. 7). Note that the V_{OC} limit of 680 mV mentioned earlier assumes zero recombination losses in the base and BSF. The implied V_{OC} data in Fig. 7 include losses in these cell regions.

C. Detailed Loss Analysis

The effects of surface recombination and bulk recombination on the V_{OC} of our cells were separated using the method shown schematically in Fig. 8. The J_0 data for the passivated phosphorous BSF from Fig. 6 (defined as J_{0B}' in Fig. 8) were first converted to S values using [32]

$$J_0 = qn_i^2 \frac{S}{N_D} \tag{2}$$

where n_i ($= 8.6\text{e}9\ \text{cm}^{-3}$) and N_D are, respectively, the intrinsic carrier concentration in silicon and the base doping density of the 3-Ω·cm wafers used for cell fabrication. The combined effect of recombination at the rear surface and recombination in the wafer bulk can be converted to a J_{0B} value using [33]

$$J_{0B} = \frac{qn_i^2}{N_D}\frac{D_p}{L_p}\frac{(SL_p/D_p) + \tanh(W/L_p)}{1 + (SL_p/D_p)\tanh(W/L_p)} \tag{3}$$

where D_P and L_P are the hole diffusivity and diffusion length, respectively, and W is the thickness of the base region. L_P was calculated from measured bulk lifetimes of oxidized test wafers which had bulk lifetimes in the range of 600–1000 μs. J_{0E}, as defined in Fig. 8, is simply the measured J_0 of the boron emitter (see Fig. 6). The sum of the J_{0B} and J_{0E} values is the J_0 ($= J_{0E} + J_{0B}$) of the one-diode model of a solar cell, allowing V_{OC} to be calculated via (1). By solving these equations, the experimental J_0 data from various steps of the cell process (see Fig. 6) were converted to V_{OC} values. These calculated V_{OC} values are plotted in Fig. 7 alongside the experimentally determined implied V_{OC}s—the two sets of data match reasonably well. This analysis validates the accuracy of the J_0 data presented in previous section and shows that almost 75% of the recombination losses in our unmetallized cells occur at the surfaces. Therefore, further improvements in surface passivation quality are required to improve the cell voltage and efficiency.

D. Cell Results

Using the process sequence described earlier which utilized a spin-on source and symmetric SiO_2/SiN_X passivation, a cell efficiency of ~20.3% (4 cm^2) was achieved using screen-printed contacts (see Fig. 9) and validated by the National Renewable Energy Laboratory.

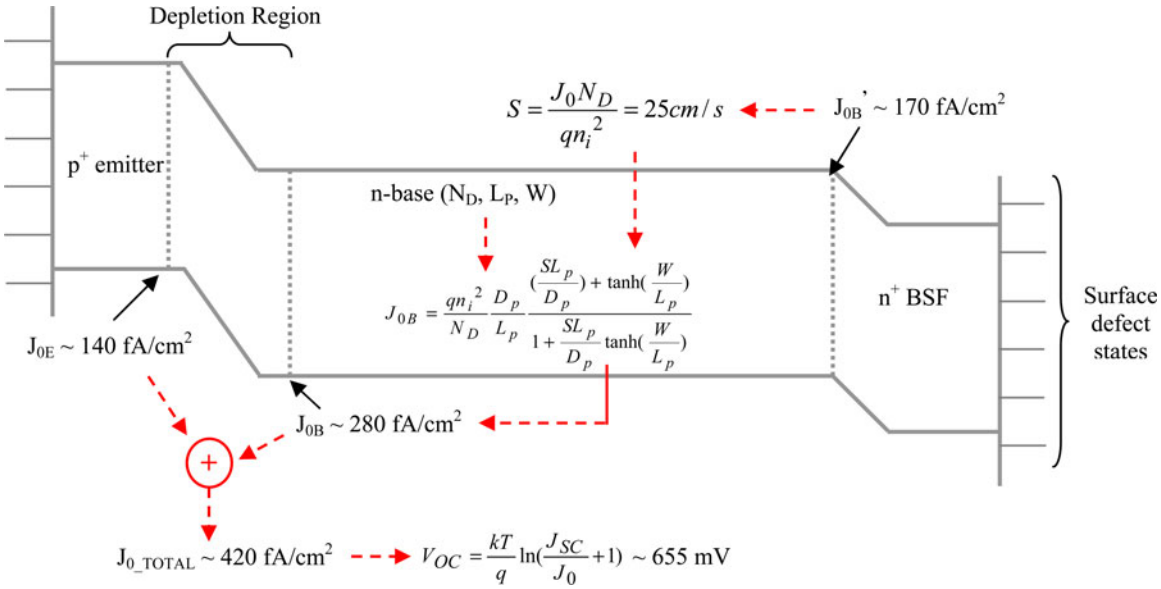

Fig. 8. Energy band diagram of an n-type cell showing the interfaces where J_{0E}, J_{0B}, and J_{0B}' are defined. The dashed arrows show the flow of equations used to convert measured J_0 values (taken from Fig. 6) and wafer parameters to a V_{OC} value (see Fig. 7).

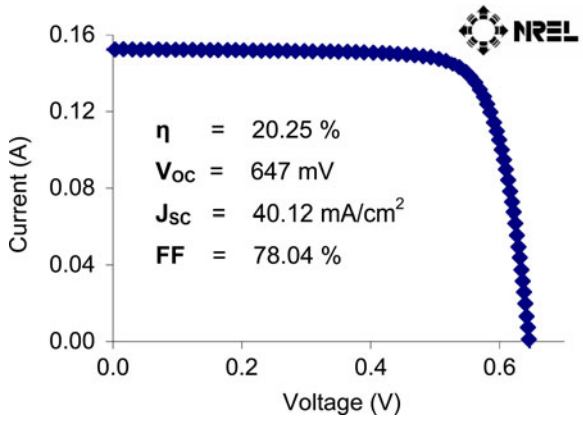

Fig. 9. *I–V* characteristics of a 4-cm^2 thermal-SiO_2/SiN_X passivated screen-printed n-type cell.

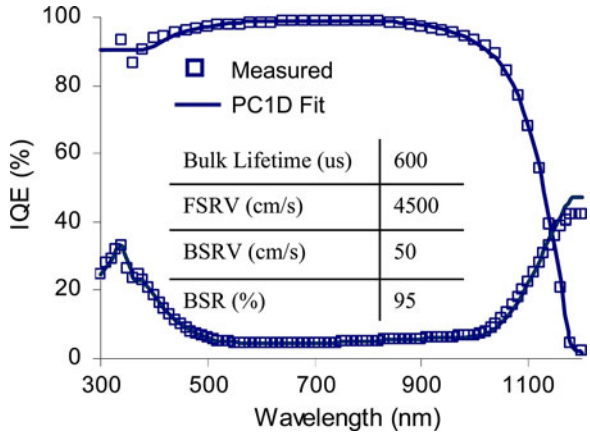

Fig. 10. PC1D fit to the IQE curve of a 20% efficient passivated n-type cell. The inset shows selected PC1D input parameters.

To our knowledge, the highest reported efficiency on non-photolithography n-type cells of the same size and using FZ Si is 20.8% achieved using an Al_2O_3-passivated emitter and inkjet printed and plated gridlines [20]. We believe that the result presented here is the second highest efficiency and the highest on n-type cells using screen-printed contacts. We also note that this n-type device which is textured on both the front and rear surfaces matches the best results that are obtained on screen-printed p-type cells which require planarization of the rear surface which adds to process complexity [16], [34], [35].

From a PC1D fit to the IQE and *I–V* characteristics of the cell (see Fig. 10), front-surface recombination velocity (FSRV) and back-surface recombination velocity (BSRV) of 4500 and 50 cm/s, respectively, were extracted along with a back-surface reflectance of 95%. Note that the BSRV extracted from PC1D is the effective rear *S* as defined in Fig. 8, while the FSRV is the *S* value at the p^+-Si surface. A comparison of Figs. 8 and 10 shows that metallization of the rear (~4% metal coverage) was sufficient to double the BSRV.

E. Stability

As noted earlier, thermal oxide passivation of p^+-Si surfaces has been found to be unstable, with a V_{OC} drop of up to 100 mV being reported on front-junction n-type PERL cells after 2–3 years of dark storage [14]. In order to test the stability of the stack passivation used here, we have tracked the *I–V* characteristics of cells that were fabricated using the process described earlier. Over a one-year period, during which the cells were stored in air in the dark, no significant degradation in *I–V* characteristics has been observed (see Table I).

TABLE I
STABILITY OF A 4-CM^2 SiO_2/SiN_X PASSIVATED SCREEN-PRINTED N-TYPE CELL

η (%)	V_{OC} (mV)	J_{SC} (mA/cm^2)	FF (%)
Initial			
19.7	648	39.0	77.95
After 1 year of dark storage in air			
19.7	647	39.3	77.56

IV. CONCLUSION

Using a spin-on boric acid diffusion source and a thin thermal SiO_2/SiN_X stack, it was found that the effects of hydrogenation, direct PECVD SiN_X deposition, and firing on surface passivation are considerably different on planar and textured p^+-Si surfaces. While SiN_X capping was found to result in a large reduction in passivation quality on planar p^+ surfaces, the opposite effect was observed on textured p^+-Si surfaces. In addition, firing the stack was found to have a larger beneficial impact on the passivation of textured samples, with a nearly fourfold reduction in J_0. This effect, in combination with the positive effect of SiN_X on oxidized textured p^+ surfaces, resulted in similar J_0 values of $\sim$150 fA/cm^2 on both planar and textured surfaces with boron surface concentrations $\sim$5e19 cm^{-3}. In addition, the fired stack provides similar passivation on both p^+- and n^+-Si surfaces with similar surface dopant concentrations. Finally, the passivation quality and stability of the thin-SiO_2/SiN_X stack, along with the suitability of a spin-on boric acid source to form a high-quality emitter, were proven at the cell level with the fabrication of a 20.25% efficient 4-cm^2 screen-printed cell.

REFERENCES

[1] J. Zhao, A. Wang, and M. A. Green, "24.5% Efficiency silicon PERT cells on MCZ substrates and 24.7% efficiency PERL cells on FZ substrates," *Prog. Photovoltaics: Res. Appl.*, vol. 7, pp. 471–474, 1999.

[2] A. Das, D. S. Kim, V. Meemongkolkiat, and A. Rohatgi, "19% efficient screen-printed cells using a passivated transparent boron back surface field," in *Proc. 33rd IEEE Photovoltaic Spec. Conf.*, 2008, pp. 1–5.

[3] D. Kray, M. Aleman, A. Fell, S. Hopman, K. Mayer, M. Mesec, R. Muller, G. P. Willeke, S. W. Glunz, B. Bitnar, D.-H. Neuhaus, R. Ludemann, T. Schlenker, D. Manz, A. Bentzen, E. Sauar, A. Pauchard, and B. Richerzhagen, "Laser-doped silicon solar cells by laser chemical processing (LCP) exceeding 20% efficiency," in *Proc. 33rd IEEE Photovoltaic Spec. Conf.*, 2008, pp. 1–3.

[4] A. Rohatgi and D. Meier, "Developing novel low-cost, high-throughput processing techniques for 20%-efficient monocrystalline silicon solar cells," *Photovoltaics Int.*, vol. 10, pp. 87–93, 2010.

[5] M. Hörteis and S. W. Glunz, "Fine line printed silicon solar cells exceeding 20% efficiency," *Prog. Photovoltaics: Res. Appl.*, vol. 16, pp. 555–560, 2008.

[6] P. P. Altermatt, J. O. Schumacher, A. Cuevas, M. J. Kerr, S. W. Glunz, R. R. King, G. Heiser, and A. Schenk, "Numerical modeling of highly doped Si:P emitters based on Fermi–Dirac statistics and self-consistent material parameters," *J. Appl. Phys.*, vol. 92, pp. 3187–3197, 2002.

[7] K. R. McIntosh and L. P. Johnson, "Recombination at textured silicon surfaces passivated with silicon dioxide," *J. Appl. Phys.*, vol. 105, pp. 124520-1–124520-10, 2009.

[8] A. G. Aberle and R. Hezel, "Progress in low-temperature surface passivation of silicon solar cells using remote-plasma silicon nitride," *Prog. Photovoltaics: Res. App.*, vol. 5, pp. 29–50, 1997.

[9] A. Rohatgi, P. Doshi, J. Moschner, T. Lauinger, A. G. Aberle, and D. S. Ruby, "Comprehensive study of rapid, low-cost silicon surface passivation technologies," *IEEE Trans. Electron Devices*, vol. 47, no. 5, pp. 987–993, May 2000.

[10] J. Schmidt and K. Bothe, "Structure and transformation of the metastable boron- and oxygen-related defect center in crystalline silicon," *Phys. Rev. B (Condensed Matter)*, vol. 69, pp. 024107-1–024107-8, 2004.

[11] A. Das and A. Rohatgi, "The impact of cell design on light induced degradation in p-type silicon solar cell," in *Proc. 37th IEEE Photovoltaic Spec. Conf.*, Jun., 2011 (in press).

[12] P. P. Altermatt, H. Plagwitz, R. Bock, J. Schmidt, R. Brendel, M. J. Kerr, and A. Cuevas, "The surface recombination velocity at boron-doped emitters: Comparison between various passivation techniques," in *Proc. 21st Eur. Photovoltaic Solar Energy Conf. Exhib.*, 2006, pp. 647–650.

[13] R. R. King, P. E. Gruenbaum, R. A. Sinton, and R. M. Swanson, "Passivated emitters in silicon solar cells," in *Proc. 21st IEEE Photovoltaic Spec. Conf.*, 1990, pp. 227–232.

[14] J. Zhao, J. Schmidt, A. Wang, G. Zhang, B. S. Richards, and M. A. Green, "Performance instability in n-type PERT silicon solar cells," in *Proc. 3rd World Conf. Photovoltaic Energy Convers.*, 2003, pp. 923–926.

[15] D. S. Kim, A. Das, K. Nakayashiki, B. Rounsaville, V. Meemongkolkiat, and A. Rohatgi, "Silicon solar cells with boron back surface field formed by using boric acid," in *Proc. 22nd Eur. Photovoltaic Solar Energy Conf. Exhib.*, 2007, pp. 1730–1733.

[16] A. Das, S. Ramanathan, A. Upadhyaya, V. Meemongkolkiat, and A. Rohatgi, "Practical challenges of achieving high efficiency boron back surface field solar cells," in *Proc. 35th IEEE Photovoltaic Spec. Conf.*, 2010, pp. 906–912.

[17] T. W. Krygowski, "A novel simultaneous diffusion technology for low-cost, high-efficiency solar cells," Ph.D. dissertation, Georgia Inst. Technol., Atlanta, 1998.

[18] J. Benick, B. Hoex, O. Schultz, and S. W. Glunz, "Surface passivation of boron diffused emitters for high efficiency solar cells," in *Proc. 33rd IEEE Photovoltaic Spec. Conf.*, 2008, pp. 1–5.

[19] B. Hoex, J. Schmidt, R. Bock, P. P. Altermatt, M. C. M. van de Sanden, and W. M. M. Kessels, "Excellent passivation of highly doped p-type Si surfaces by the negative-charge-dielectric Al_2O_3," *Appl. Phys. Lett.*, vol. 91, pp. 112107-1–112107-3, 2007.

[20] A. Richter, S. Henneck, J. Benick, M. Hörteis, M. Hermle, and S. W. Glunz, "Firing stable Al_2O_3/SiN_X layer stack passivation for the front side boron emitter of N-type silicon solar cells," in *Proc. 5th World Conf. Photovoltaic Energy Convers.*, 2010, pp. 1453–1459.

[21] V. D. Mihailetchi, J. Jourdan, A. Edler, R. Kopecek, R. Harney, D. Stichtenoth, J. Lossen, T. S. Böscke, and H.-J. Krokoszinski, "Screen-printed n-type silicon solar cells for industrial application," in *Proc. 5th World Conf. Photovoltaic Energy Convers.*, 2010, pp. 1446–1448.

[22] T. Desrues, J. Jourdan, Y. Veschetti, and R. Monna, "N-type Si solar cells with B-doped emitter using spin-on dopants (SOD)," *Proc. 22nd Eur. Photovoltaic Solar Energy Conf. Exhib.*, 2007, pp. 1209–1212.

[23] M. J. O'Neil, Ed., *The Merck Index*, 14th ed., Whitehouse Station, NJ: Merck, 2006.

[24] S. K. Ghandhi, *VLSI Fabrication Principles: Silicon and Gallium Arsenide*, 2nd ed. New York: Wiley, 1994.

[25] A. Das and A. Rohatgi, "Optical and electrical characterization of silver microflake colloid films," *J. Electrochem. Soc.*, vol. 157, pp. H301–H303, 2010.

[26] A. Cuevas and R. A. Sinton, "Prediction of the open-circuit voltage of solar cells from the steady-state photoconductance," *Prog. Photovoltaics: Res Appl.*, vol. 5, pp. 79–90, 1997.

[27] D. E. Kane and R. M. Swanson, "Measurement of the emitter saturation current by a contactless photoconductivity decay method," in *Proc. 18th IEEE Photovoltaic Spec. Conf.*, 1985, pp. 578–583.

[28] S. L. Elliot, R. F. Broom, and C. J. Humphreys, "Dopant profiling with the scanning electron microscope: A study of Si," *J. Appl. Phys.*, vol. 91, pp. 9116–9122, 2002.

[29] V. Yelundur, A. Rohatgi, J. I. Hanoka, and R. Reedy, "Beneficial impact of low frequency PECVD SiN_X:H-induced hydrogenation in high-efficiency string ribbon silicon solar cells," in *Proc 19th Eur. Photovoltaic Solar Energy Conf. Exhib.*, 2004, pp. 951–954.

[30] B. Sopori, R. Reedy, K. Jones, L. Gedvilas, B. Keyes, Y. Yan, M. Al-Jassim, V. Yelundur, and Ajeet Rohatgi, "Damage-layer-mediated H diffusion during SiN:H processing: A comprehensive model," in *Proc. 4th World Conf. Photovoltaic Energy Convers.*, 2006, pp. 1028–1031.

[31] M. Sheoran, D. S. Kim, and A. Rohatgi, "Hydrogen diffusion in silicon from PECVD silicon nitride," in *Proc. 33rd IEEE Photovoltaic Spec. Conf.*, 2008.

[32] R. R. King, R. A. Sinton, and R. M. Swanson, "Studies of diffused phosphorus emitters: Saturation current, surface recombination velocity, and quantum efficiency," *IEEE Trans. Electron. Devices*, vol. 37, no. 2, pp. 365–371, Feb. 1990.
[33] M. A. Green, *Solar Cells: Operating Principles, Technology and System Applications*. Sydney, Australia: Univ. New South Wales, 1998.
[34] S. Ramanathan, V. Meemongkolkiat, A. Das, A. Rohatgi, and I. Koehler, "Fabrication of 20% efficient cells using spin-on based simultaneous diffusion and dielectric anneal," in *Proc. 34th IEEE Photovoltaic Spec. Conf.*, 2009, pp. 2150–2153.
[35] J.-H. Lai, A. Upadhyaya, S. Ramanathan, A. Das, K. Tate, V. Upadhyaya, A. Kapoor, C.-W. Chen, and A. Rohatgi, "High-efficiency large-area rear passivated silicon solar cells with local Al-BSF and screen-printed contacts," *IEEE J. Photovoltaics*, vol. 1, no. 1, 2011.

Arnab Das received the B.S. degree in computer engineering in 2004 from the Georgia Institute of Technology, Atlanta. He then joined the University Center of Excellence for Photovoltaics, Georgia Institute of Technology, where he is currently pursuing the Ph.D. degree in electrical engineering.

His current research interests include the fabrication and characterization of silicon photovoltaic devices with emphasis on surface passivation and optical trapping.

Kyungsun Ryu received the B.S. degree in electrical engineering from Korea University, Seoul, Korea, in 2007 and the M.S. degree in electrical engineering from Columbia University, New York, NY, in 2009. He is currently working toward the Ph.D. degree in electrical and computer engineering with Georgia Institute of Technology, Atlanta.

His research interests include the fabrication and characterization of n-type crystalline silicon solar cells.

Ajeet Rohatgi (F'08) received the B.S. degree in electrical engineering from the Indian Institute of Technology, Kanpur, India, in 1971, the M.S. degree in materials engineering from the Virginia Polytechnic Institute and State University, Blacksburg, in 1973, and the Ph.D. degree in metallurgy and material science from Lehigh University, Bethlehem, PA, in 1977.

He is a Regents' Professor and a Georgia Power Distinguished Professor with the School of Electrical Engineering. He is the founding director of the University Center of Excellence for Photovoltaic Research and Education at the Georgia Institute of Technology, Atlanta, and the Founder and CTO of Suniva Inc. Before joining the Electrical Engineering faculty at the Georgia Institute of Technology in 1985, he was a Westinghouse Fellow with the Research and Development Center, Pittsburgh, PA. His current research interests include the development of cost and efficiency roadmaps for attaining grid parity with Silicon PV, understanding of impurity effects in silicon solar cells, gettering and passivation of defects in solar grade silicon, rapid thermal processing of solar cells, the design and fabrication of low-cost, high-efficiency cells on mono and multicrystalline silicon, and the design, performance, and economics of photovoltaic systems.

Dr. Rohatgi has published over 370 technical papers in this field and has been awarded 11 patents. He is on the editorial board of several PV publications and served as general chair for the 28th IEEE Photovoltaic Specialists Conference in Alaska in 2000. He received the Westinghouse Engineering Achievement Award in 1985 and the Georgia Institute of Technology Distinguished Professor Award in 1996 for his research on high-efficiency solar cells. In 2003, he received the IEEE PVSC William Cherry Award and the National Renewable Energy Laboratory/Department of Energy Rappaport Award for his contributions to photovoltaics. In 2007, he received the Georgia Institute of Technology Outstanding Research Program Development Award. In 2008, he was recognized as one of the five most influential people in renewable energy by *Power Finance & Risk Magazine*, as well as by the Georgia Sierra Club, for his efforts to help move both Georgia and the U.S. into a clean energy economy through his solar energy research at the Georgia Institute of Technology. In 2009, he received the Envention Award for conservation and pollution-curbing efforts from the Atlanta Business Chronicle, the Climate Protection Award for dedication and technical innovation in photovoltaics from the Environmental Protection Agency, and the Hoyt Clark Hottel Award for outstanding educator and innovator in the field of photovoltaics from the American Solar Energy Society.